Color tunability of organic light emitting devices through Singlet oxygen exposure of chemical dopants

An honors thesis for

The Department of Chemical & Biological Engineering.

By

Sanya T. Ramjattan

Tufts University 2012.

ACKNOWLEDGEMENTS

This thesis was facilitated by various persons and groups who have been actively involved in the shaping and direction of its outcomes. Firstly, I must extend my sincerest thanks to my research advisor and personal mentor, Professor Matthew Panzer whose continued support has been most accommodating. His expert advice and keen observations were infinitely helpful in times of difficulty and I am indebted to him for allowing me to conduct such intriguing research in his laboratory group.

I am grateful also to Professor Samuel Thomas of the Tufts Chemistry Department who graciously provided all the emissive polymeric materials used in the experiments as well as insightful contributions to the course of experiments. The final member of my thesis committee, Professor of the Practice: Derek Mess, has been a vital asset in molding my undergraduate research experience and helping me realize my true potential. I thank him profusely for his encouragement.

It is not without the assistance of Dr. Damla Koylu of the Thomas lab that I have procured key materials to utilize in the lab. She has been an important resource for these experiments and her time and efforts are greatly appreciated. Fellow group members of the Panzer lab were also quite helpful and I take this opportunity to thank Adam Visentin and Athina Pantelidou for their patience, guidance and instruction during the initial stages of this endeavor.

I must express my sincerest appreciation to the Tufts Summer Scholars Program and the Department of Chemical and Biological Engineering. This thesis originated from a Summer Scholars project which was generously funded by a prestigious grant, without which, the

project would not have been possible. I thank the members of our department for their help with printing of posters and manuscripts as well as administrative affairs. Finally, my thanks to the friends and family members who encouraged me to continue with an honors thesis and to pursue my research interests.

TABLE OF CONTENTS

LIST OF FIGURES

LIST OF TABLES

ABSTRACT

Display technologies are rapidly developing to match consumer needs and manufacturers are becoming more interested in organic light emitting devices (OLEDs) as they are promising candidates for flexible displays and light-weight, transparent devices. This research involved the fabrication and optimization of novel OLEDs incorporating doped photo-emissive polyfluorenes, with the specific goal of achieving patternable devices for economic manufacture. The experimental methods employed are less energy intensive and more amenable to flexible applications than those for most inorganic LEDs. Devices synthesized with a blue-emitting polyfluorene and doped with green, amber and red emitting acenes have been characterized. The electroluminescent stability and color tunability of dopant endoperoxides have also been investigated. Doping was found to increase external quantum efficiency by two orders of magnitude; the trend in efficiency mirrored the degree of overlap between dopant absorption and host emission. Oxidation of acenes to form the endoperoxide produced electroluminescent spectra which exhibited different color and stability characteristics from un-oxidized devices. Evidence of the polyfluorene host was present in peroxide spectra but not in doped device spectra, indicating that oxidation successfully deactivated dopants and achieved color tunability. The exception was pentacene peroxide devices which became more stable after treatment and demonstrated high efficiency but no change in color.

1. INTRODUCTION

1.1. OVERVIEW

As global interest in cleaner energy and sustainable lifestyles grows, there is constant improvement in solid state lighting and display technologies towards more efficient, higher quality and increasingly durable designs. Light emitting devices (LEDs), particularly OLEDs, play an important role in this progression. They are attractive replacements for compact fluorescent lights (CFLs) and liquid crystal displays (LCDs), which are predominantly employed in today's lighting and display technologies respectively [1].

OLEDs offer promising alternatives to CFLs and LCDs because of their potential for flexible applications – a recent development that is becoming increasingly viable due to concurrent developments in flexible transistors [2]. They are also appropriate for thin film, lightweight displays since they can be fabricated using unique printing or spin-coating techniques [2], [3]. Other advantageous characteristics of OLEDs include high efficiency, low cost, increased viewing angle, high contrast and the ability to self-emit as opposed to LCDs which require backlighting [1].

Such characteristics have piqued interest in OLEDs on the research and development level as well as in commercial manufacturing. DisplaySearch, a leading firm in market research for global display supply chains, projected the compound annual growth rate of OLEDs in this sector to be 20% [4]. Furthermore, forecasted estimates for the growth of OLED televisions were over 120% as shown in Table 1.1.1 below.

Table 1.1.1 – Compound Annual Growth Rates for OLED and OLED TVs [4]

Application	2008/millions $	CAGR (2001-2008)	CAGR (2008-2015)
OLED	83.5	85%	20%
OLED TV	0.0	0%	126%

Currently, the most significant barrier to the large scale realization of OLEDs is the prohibitive manufacturing costs incurred by extensive research and development in optimizing performance. Cost has been a primary barrier for example, in the large scale realization of the OLED TV.

1.2. Historical Perspective

The first 'efficient' OLEDs, pioneered by VanSlyke and Tang in 1987 at the Kodak Company, had reported external quantum efficiencies [See Section 1.3] of 1% and comprised of a thin-film multilayer cell [5]. An organic electroluminescent layer, comprising 8-hydroxyquinoline aluminum (Alq3) and an aromatic diamine, was deposited between indium tin oxide (ITO) and Mg:Al electrodes. This layered structure was the premise for several other device architectures to follow.

Researchers incorporated additional layers with specific roles to enhance the device performance. Amongst these were the hole injection layer (HIL), hole transport layer (HTL), hole blocking layer (HBL) and electron transport layer (ETL). Figure 1.2.1 illustrates this evolution. Current devices typically use an ITO transparent electrode, metal opaque electrode and poly(3,4-ethylenedioxythiophene):poly(styrenesulfonate) (PEDOT:PSS) as the hole injection layer [6]. Each additional development has brought OLED technology closer to large scale implementation and has expanded the range of potential applications.

Figure 1.2.1 - Evolution of General OLED structure [1]

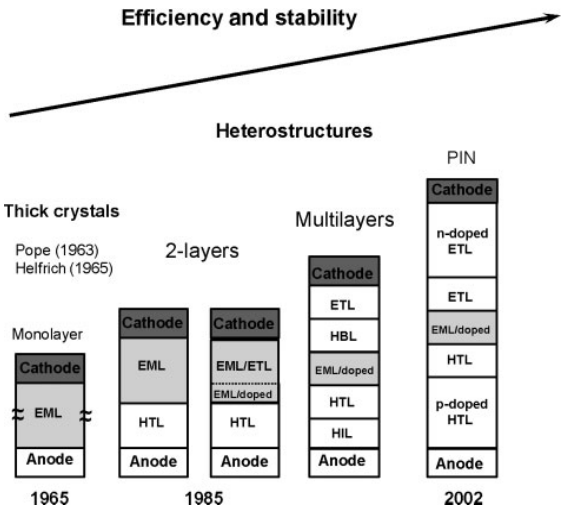

1.3. MATERIALS

With reference to the multi layered structure outlined in Figure 1.2.1, the format used for these experiments involve an ITO transparent anode, PEDOT:PSS HIL, 1,3,5-Tris(1-phenyl-1H-benzimidazol-2-yl)benzene (TPBi) ETL and calcium/silver electrodes. The primary emissive polymer used was a commercial blue-emitting polyfluorene, poly(9,9-di-n-dodecylfluorenyl-2,7-diyl), P1. It has been utilized in other works to produce blue OLEDs [7], and it is a good candidate for doping due to the wide band gap associated with its blue emission [8].

Three dopants were investigated in this research, including green emitting 5,12-bis(4-methoxyphenyl)tetracene, herein referred to as tetracene, rubrene (amber emitting) and red emitting 6,13-bis(4-methoxyphenyl)pentacene, referred to as pentacene. The structures of these organic compounds are shown below.

Figure 1.3.1 - Organic Compounds Used in Experiments

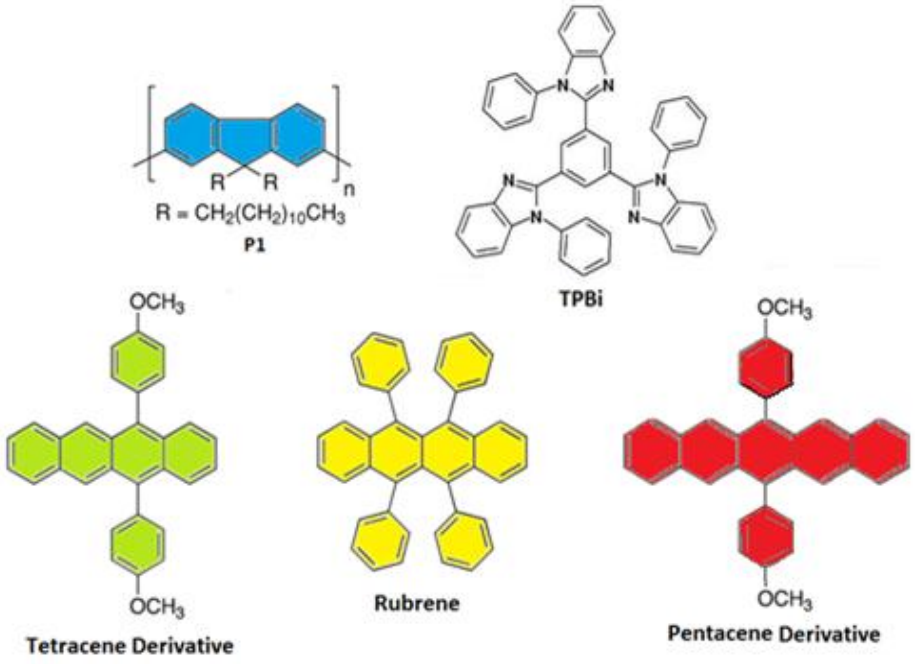

All three dopants (tetracene, rubrene and pentacene) are capable of forming the associated endoperoxide [Figure 1.3.2] via simultaneous UV irradiation and singlet oxygen exposure [9]. The endoperoxides are not chromophores, as the conjugated pi systems originally present in the acenes have been disrupted by the peroxide bond. Consequently, upon generation of the endoperoxide, the color of light produced should revert to that of the pure P1 host, showing no influence from the dopant. This provides the basis for the color tunability of OLEDs presented in this research.

Figure 1.3.2 - Acene Endoperoxides

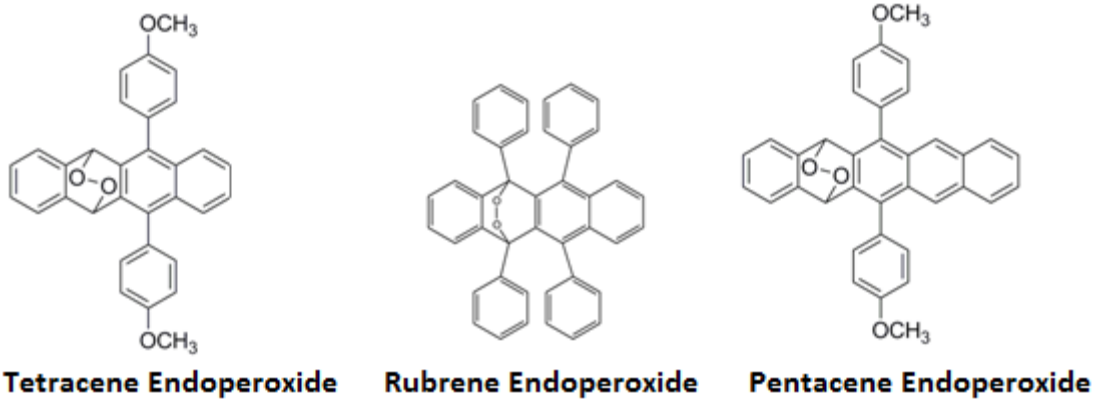

P1 is also known to undergo some degradation under prolonged exposure to air. Thus, polymeric material and dopants from these experiments require an inert nitrogen environment during deposition and evaluation.

1.4. BACKGROUND

When a voltage is applied across the layered format illustrated in Figure 1.2.1, electrons and holes flow through the device. Figure 1.4.1 shows the energy band diagram that is established for OLEDs fabricated in this research.

Figure 1.4.1 - Energy Band Diagram for Fabricated OLEDs [7] [15] [16]

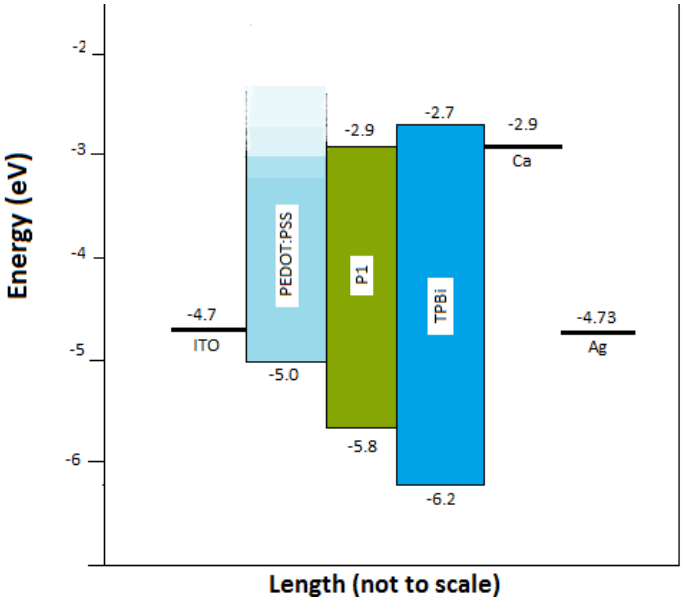

Electrons flow in through the metallic cathode and are transported through the TPBi ETL while holes enter through the ITO anode and travel through the PEDOT:PSS layer. At the emissive layer, electron-hole pairs or excitons, recombine to produce light if the applied voltage is greater than the turn on voltage (V_t). Such operation lends to the characteristic diode behavior, shown in Figure 1.4.2, which is commonly exhibited by OLEDs.

The color of emitted light is directly related to the band gap (represented by difference between the HOMO and LUMO) of the organic emitter which can be varied by altering the structure of the emissive compound. Additionally, doping has been known to modify the color of light produced as well as increase the performance of OLEDs. Such influence arises from Förster resonant energy transfer between organic hosts with larger band gaps to dopant compounds with smaller band gaps [Appendix A].

Figure 1.4.2 - Characteristic I-V Plot for Diode Behavior

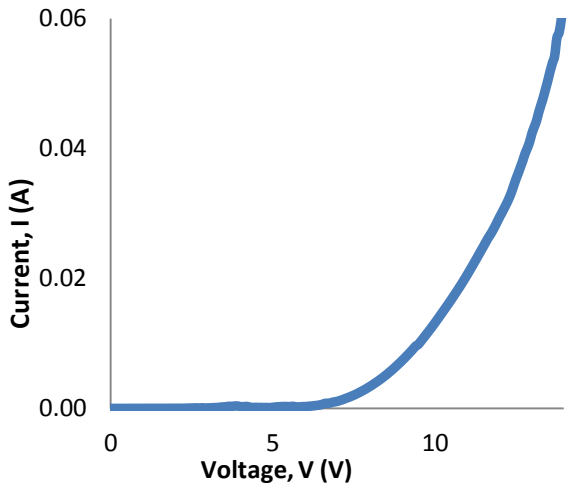

The general performance of LEDs can be gauged by their quantum efficiency both internal (IQE) and external (EQE). The former is a ratio of the total radiative to non-radiative exciton- recombinations. EQE is a measure of the quantity of photons emitted to the net current through the device. For light at a single wavelength, the monochromatic EQE can be estimated by [10]:

$$\text{EQE\%} = 100 \cdot g \cdot W \cdot \frac{\lambda}{h \cdot c} \cdot \frac{q}{i} \qquad \text{[E-1]}$$

g – geometric factor

h – Planck's constant

c – speed of light

λ – wavelength of emitted light

q – fundamental electron charge

i – current through device

W - luminous power out at current, i

The organic emitters herein investigated exhibit fluorescence, in which paired ground state electrons undergo photo-excitation to the singlet excited state (retaining spin) and

subsequently relax to the singlet ground state. As previously stated, electric stimulation can also cause excited electrons to relax to the singlet state through radiative recombination. Statistics dictate that for every singlet excited state produced, three triplet states (excited electron shares spin with ground state electron) are generated as well [Appendix A]. Consequently, organic semiconductors which solely demonstrate fluorescence, demonstrate maximum internal quantum efficiency of 25% [11].

Another point of interest for the quality of OLEDs is the electroluminescent (EL) spectrum which graphs the intensity of emission across the visible spectrum. It is worth emphasizing that organic compounds produce broad peaks in their EL spectra whereas inorganic emitters generate sharper peaks. UV-Vis absorbance spectra for the three acenes are depicted in Figure 1.4.3 together with the representative EL spectrum of P1.

Figure 1.4.3 - Absorption Spectra of Dopants in Dichloromethane

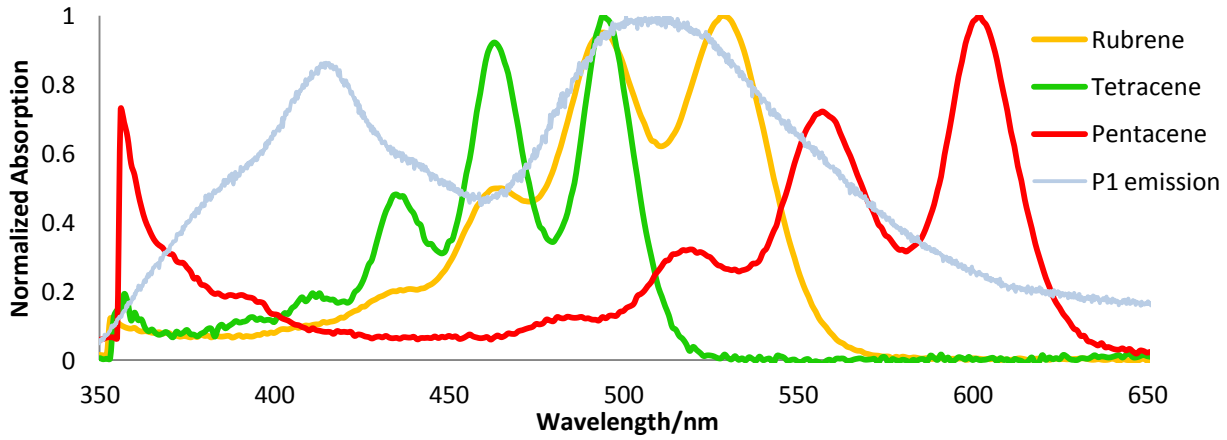

The relative efficiencies of doped OLEDs may be gauged by the degree of overlap between host emission and dopant absorption [12]. From Figure 1.4.3, we can expect rubrene devices to perform best as the absorption spectrum coincides significantly with the primary P1

emission peak centered at 510nm. Tetracene OLEDs should demonstrate comparable performance while pentacene devices should yield lower EQE by this logic.

1.5. OBJECTIVES

In this research, we seek to develop a cost effective means of fabricating patternable OLEDs with post-deposition color tunability. Utilizing a polyfluorene host for acenes and their corresponding endoperoxide dopants, the emissive layers for OLEDs were varied to investigate both their efficiency and spectral responses.

Of particular interest is the effect of oxidizing doped films via UV light and singlet oxygen exposure, to generate endoperoxides. This process can modify color characteristics without supplanting the emissive layer entirely but by post-deposition UV treatment. Electronic excitation of the endoperoxide doped films is expected to sever the peroxide bonds and regenerate the un-oxidized doped film.

We seek to verify this by investigating the spectral responses of UV-treated, doped OLEDs. Three phases of experiments were conducted: pure P1 devices, doped P1 OLEDs and peroxide doped P1 devices. This thesis presents the findings from all experimental phases and the conclusions which can be drawn. I have also included suggestions for areas of future work which may be explored by interested parties.

2. Experimental Methods

2.1. Pre-Deposition Treatment

Glass substrates (1"x 1") patterned with ITO were pre-manufactured and ordered in bulk (Thin Film Devices Inc.). These were rigorously cleansed prior to any depositions using a four stage process. Four designated 150ml beakers, each reserved for soap, de-ionized water, acetone and isopropyl alcohol (IPA), were required for this treatment. First, substrates were sonicated in 0.2% Micro 90 soap for 5 minutes and then in deionized water for another 5 minutes. This was followed by sonication in acetone for 5 minutes and then a boiling IPA soak for 5 minutes on a hot plate with set-point of 130°C. Upon removal from the IPA bath, substrates were dried with nitrogen gas to prevent streaking and then placed face-down in labeled polypropylene holding cases (Fluoroware Inc.).

Following the cleaning process, substrates were subjected to oxygen plasma treatment for 1 minute to render the surface more hydrophilic in preparation for spin coating. All devices made subsequent to 6/17/2012 underwent an alternative surface treatment involving a 30 minute 1M NaOH soak instead.

Figure 2.1.1 - Pre-Deposition Substrate Treatment

2.2. FABRICATION

All OLEDs made followed the format ITO/PEDOT:PSS(3000rpm)/emissive polymer/TPBi/Ca(40nm)/Ag(60nm) as outlined in Figure 2.2.1.

Figure 2.2.1 - Device Architecture for Fabricated OLEDs

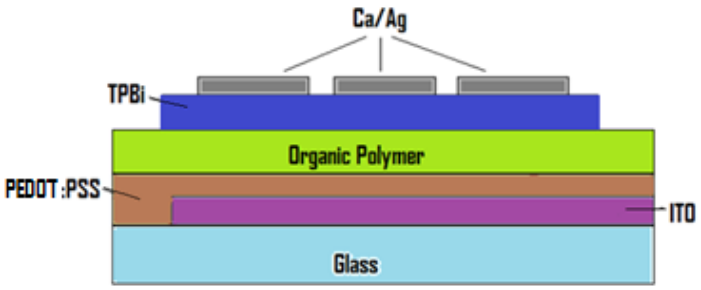

OLEDs were made in a 3 stage process involving PEDOT:PSS deposition, emissive layer deposition and thermal evaporation under vacuum of three final layers.

The first deposited layer was the HIL, which was performed via spin-coating in air. PEDOT:PSS solution was transferred onto the substrate through a 3ml disposable syringe with an attached 0.45µm PTFE filter (Millipore) and then spun onto the surface using the Laurel Technologies spin-coater (WS-400BZ-6NPP/LITE) in the fume hood at 3000rpm for 60s. Substrates were then baked (face-up) on a hot plate set to 120°C for 10 minutes.

After PEDOT:PSS deposition, substrates were loaded into the left glove box for deposition of the emissive layer in nitrogen. Once again, solutions were transferred onto the substrate surface with a 3ml syringe through a PTFE filter. The spin speed was varied for different experiments but remained in the range of 1000rpm to 5000rpm for 60s. Emissive solution composition varied by experiment, maintaining the P1 host concentration at 20mg/ml. Solutions of 2% and 10% dopant by weight were prepared using 2.0ml of host solution

with 0.2ml and 1.0ml of 4mg/ml dopant/toluene solution respectively[1]. All P1 and dopant material were obtained from the Thomas Lab. Following spin-coating, devices were left in their holding cases in the middle chamber of the glove boxes, which was pumped down to -30inHg for 30 minutes. The pump valve was then closed and the chamber was left at that pressure for 24 hours.

To investigate the color tunability of the doped devices, 2% doped emissive films spun at 3000rpm were UV irradiated in air for 5-7minutes. After the color of fluorescence of the film reverted to blue due to deactivation of the dopant to the corresponding endoperoxide, UV irradiation was continued for at least two more minutes, ensuring that both faces of the substrate were equally exposed to the light. Substrates were then reloaded into the glove box for deposition of the remaining components. A parallel set of devices was fabricated using 2% solutions of the endoperoxide also spun at 3000rpm.

For the final three layers of the OLED thermal evaporation under vacuum was employed. Deposition of the ETL, TPBi, was performed on a loading base for 4 substrates, through a custom stainless steel mask [Appendix B]. The thickness of this layer varied by experiment but was kept within 20nm – 60nm. The metal electrodes, comprising calcium and silver were sequentially added through a separate custom mask [Appendix B], producing 6 distinct pads per device for independent testing. Calcium was first evaporated to a thickness of 40nm followed by 60nm of silver.. Layer thickness was monitored within the vacuum chamber by a quartz crystal monitor (Inficon SQM 160) calibrated for each material. Figure 2.2.2 is a schematic of a completed device.

[1] Pentacene solutions were approximate 2% and 10% weight composition due to limited solubility in toluene at room temperature. Pentacene doped OLEDs are henceforth referred to as 2*% and 10*%.

Figure 2.2.2 - Completed OLED Schematic

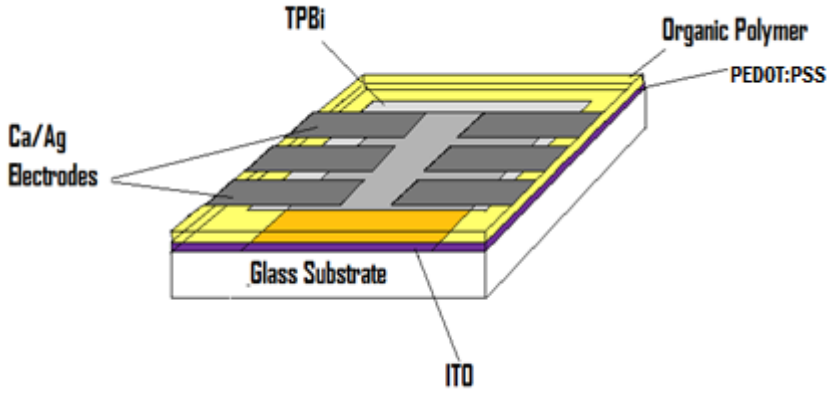

2.3. ASSESSMENT

Device testing consisted of two components: I-V sweeps with simultaneous photodiode recording and spectral acquisition at fixed voltage. To facilitate an applied voltage across the device electrodes, substrates were loaded into a customized testing apparatus used previously for photovoltaic testing [Appendix B]. At the point of contact with the anode pin, the surface of the OLED was scratched to remove deposited material and thus allow direct contact with the underlying ITO layer.

All testing was performed in the glove boxes after 19/07/2011. Previous devices were tested in a nitrogen-filled enclosure outside of the glove boxes. Voltage was applied through the Keithley 2602A System Sourcemeter in a constant sweep from 0V to a variable final voltage in the range of 14V – 20V while a photodiode detector (S120VC ThorLabs) connected to a power meter console (PM100D) measured the light power output as a function of time. After each pad was tested, the detector was manually repositioned over the new pad to optimize light detection. EL spectra were acquired using an Ocean Optics spectrophotometer (USB4000) in the glove box. Voltages and integration times differed by device.

Although the morphology of spun films was not a critical factor in this research, atomic force microscopy (AFM) was employed during preliminary stages to estimate the thickness of films. All AFM images were captured in air, from already tested OLEDs and the only information extracted was film thickness.

2.4. DATA ANALYSIS

External quantum efficiency values for each evaluated pad were calculated using [E-1] with the geometric factor, g set to 1. W is luminous power out (minus the background reading) at the single value of final current obtained from the I-V sweep and λ was selected based on the peak wavelengths observed in the EL spectra. Here, average EQE will be frequently reported alongside standard deviation and the number of pads (6 per device) used for analysis since all 6 pads did not always provide usable data.

For qualitative comparison of color attributes and color stability, EL spectra from several devices were normalized and plotted on the same graphs. The spectral variation with time was also investigated for the doped peroxide devices.

3. Results and Discussion

The results from all experiments are illustrated in summary by Appendix C.

3.1. Undoped P1

The first generation OLEDs fabricated in this research comprised P1 emissive layers with two manipulated variables in independent experiments: spin speed (ω) of P1 and thickness of TPBi. For varying spin speed, the TPBi layer was maintained at 40nm and it was expected that the emissive layer thickness, δ, would vary as:

$$\delta \propto \frac{1}{\sqrt{\omega^2}} \qquad \text{[E-2]}$$

The results are summarized below[2]. Average EQE is reported with standard deviation and the number of data points used to estimate these values.

Table 3.1.1 - Summary of P1 OLEDs Performance

P1 Spin Speed	TPBi Thickness/nm	Avg EQE% [std. dev; #points] at λ=450nm	Turn on voltage/V ± 1V	Peak Wavelength/nm
2000	40	2.29E-4 [9.1E-6; 4]	8-9	510
3000	20	2.45E-4 [3.4E-5; 5]	5.5-7	
	40	2.41E-4 [2.6E-5; 4] 7.52E-4 [4.4E-4; 2][3]	7-7.5	
	60	11.0E-4 [3E-4; 5]	7-9.5	
4000	40	3.65E-4 [3.1E-5; 6]	7	
5000	40	6.35E-4 [1]	6.5	

[2] In this preliminary set of experiments involving manipulation of P1 solution spin speed, testing was conducted outside the glove box in the nitrogen filled testing enclosure. EQE values are particularly low as a result of losses through the enclosure.

[3] Data set obtained in second set of experiments wherein testing was performed in the glove box. EQE was therefore higher.

Figure 3.1.1 - EQE Dependence on P1 Spin Speed

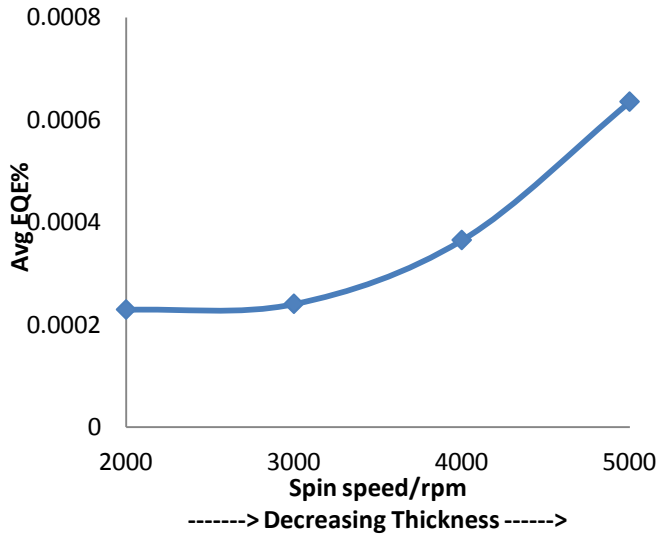

Table 3.1.2 - P1 Layer Thickness with Varying Spin Speeds

Spin Speed/rpm	Approximate Thickness/nm
1000	65
3000	40
4000	25
5000	10

Table 3.1.2 provides the approximate thickness of the P1 film as estimated by AFM for devices fabricated at different spin speeds. It was found that the estimated thicknesses did not fully subscribe to the correlation shown in E-2. While linearity was achieved with the three fastest speeds, the regression did not pass through the origin, indicating that some experimental offset may be present.

The general trend shown in Figure 3.1.1 suggests that devices perform better with thinner emissive layers. Increased electron flow due to reduced resistance of thinner films could generate more electron-hole pairs, potentially boosting efficiency. It is hypothesized that this contributes to the observed upward trend of Figure 3.1.1. Additionally, radiative emission may be hindered by thick emissive layers as the likelihood of exciton recombination across a relatively large distance is reduced. This could also account for the observed lower EQE of the thicker OLEDs.

Excessively thin films however, may contain morphological defects which can result in pinholes [13] and therefore cause poor performance characteristics. For example, despite

the highest EQE of above 0.0006% for the 5000rpm device, this speed was not implemented in further experiments as only 1 of 6 pads worked when turned on. Although this single pad functioned more efficiently than other devices, it was inferred that the deposited film was too non-uniform to be of any practical use in future experiments.

In varying TPBi thickness, the P1 spin speed was kept at 3000rpm (maintaining all other parameters at the specified values of Section 2.2)[4]. An opposing trend was observed for varying ETL thickness: thinner layers yielded lower average EQE [Figure 3.1.2]. As this component of the device structure is not directly associated with exciton generation, this progression may be explained solely by the current flow through the device. Theoretically, thinner layers would result in higher current density through the device, since overall resistance decreases. This translates to diminished EQE according to the relation outlined in equation E-1 and offers some insight to the observed behavior in Figure 3.1.2.

Figure 3.1.2 - EQE Dependence on TPBi thickness

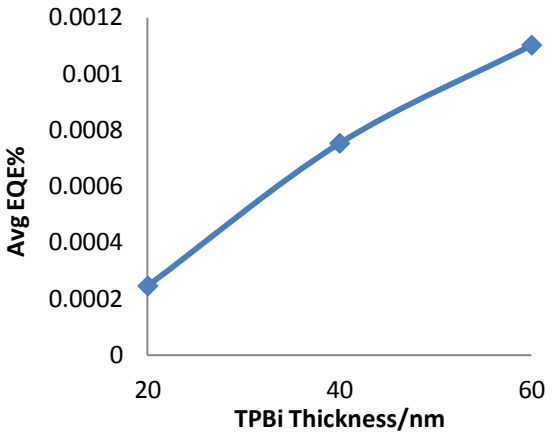

There was a general inclination for turn on voltage, V_t, to increase with device thickness. As spin speeds for the emissive layer increased (hence thickness *decreased*), or as TPBi thickness decreased, V_t was observed to diminish as well. Such behavior is expected as V_t corresponds closely to the net energy required to move charge across the entire device in order to generate light. For thicker devices, this energy is generally higher.

[4] TPBi dependence experiments (and all experiments thereafter) were conducted by testing EQE *inside* the glove box and as such EQE was noticeably higher for these OLEDs compared to those in the preceding P1 thickness dependence experiment.

The EL spectrum of an undoped P1 device (spun at 3000rpm with 60nm TPBi) is shown in Figure 3.1.3. There was minimal variation in the spectrum for changing TPBi thickness and P1 spin speed. The peak wavelengths occurred at 415nm and 510nm.

Figure 3.1.3 - Characteristic P1 EL Spectrum

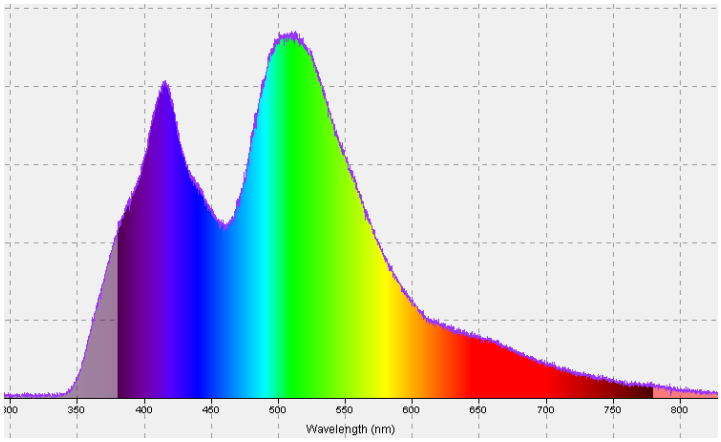

While time dependence of the EL spectra was not analyzed, the color of undoped P1 was initially purple-blue but faded to a pale green with time. These devices were not very stable with time and within 1-2 minutes of light emission, underwent noticeable dimming, color degradation as mentioned above, and quite frequently, pad extinction at high voltages.

3.2. Doped P1

Four different configurations were used for analysis of dopant influence: 2% and 10% emissive solutions each with either 40nm or 60nm TPBi, holding all other parameters at the specifications outlined in Section 2.2. Spin coating was done at 3000rpm. The 2% films were anticipated to be thinner compared to the 10% films, due to the diminished solute content. EQE enhancement was expected from doping in general, due to Förster resonant energy transfer from the larger band gap host to smaller band gap dopants [Appendix A]. Indeed, the reported EQE for all doped OLEDs was greater than that of undoped P1 devices. They were also more stable with time in terms of color and life span, particularly the pentacene doped devices. Figure 3.2.1 provides representative spectra for each of the 2%

doped OLEDs with 40nm TPBi. For the three investigated acenes, the acquired EL spectra varied minimally.

Figure 3.2.1 – Characteristic EL Spectra of 2% Doped OLEDs

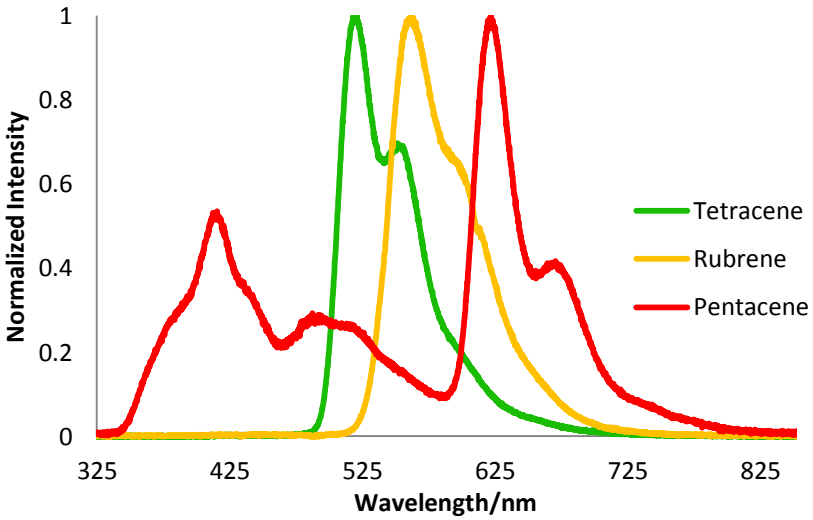

Rubrene

It was found that two recipes worked particularly well for rubrene: 2%:60nm and 10%:40nm. Both devices had calculated efficiencies of roughly 0.12%, an increase from undoped efficiency by two orders of magnitude. Table 3.2.1 summarizes the average EQE [standard deviation; number of data points used in calculation], peak wavelength and approximate turn on voltages for rubrene doped OLEDs.

Table 3.2.1 - Summary of Rubrene Doped OLEDs Performance

TPBi Thickness	**40nm**	**60nm**
Average EQE% [std dev; # data pts] at λ=560nm		
2%	0.0391 [0.005; 2]	**0.1195 [0.018; 4]**
10%	**0.1218 [0.009; 5]**	0.0224 [0.022; 4]
Turn on Voltage/V ± 1V		
2%	7-9	9
10%	8-9	7-9
Peak Wavelength:	**562nm**	

The improved performance of the 2%:60nm and 10%:40nm OLEDs may be attributed to the final thickness of these devices. The combination of a thinner 2% emissive film with a thicker ETL or a thicker 10% emissive film with a thinner ETL could yield a final device architecture of optimal thickness. Further work investigating the nature of the spun films is required.

The turn on voltage for rubrene devices were slightly higher than the corresponding undoped P1 recipe. This could be due to a change in the interaction of the emissive layer with its neighboring layers or the overall resistance of the device increasing therefore producing a more significant voltage drop across the emissive layer.

Figure 3.2.2 - Rubrene Doped OLED EL Spectrum

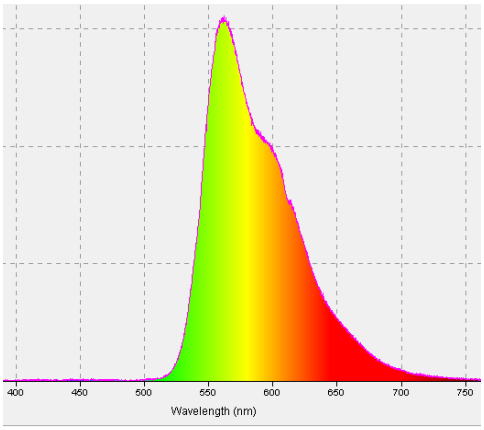

The EL spectrum for rubrene contains no remnants of the P1 host emission but rather displays emission primarily in the yellow region. This suggests that there is near complete energy transfer from the blue host to the rubrene dopant, as expected. Due to the overlap of rubrene's absorbance spectrum with P1 emission shown in Figure 1.4.3, there is considerable energy transfer to the dopant[5]. In fact the reported EQE for rubrene OLEDs was generally the highest of the three sets of doped devices. There were no discernible differences between the spectra for the four recipes investigated for rubrene.

[5] The absorbance spectra provided in Figure 1.4.3 pertain to rubrene in dichloromethane solution whilst toluene was used to make the dopant solutions in these experiments. Thus, absorbance spectra offer a qualitative comparison.

Tetracene

While the same recipes yielded the highest EQE for tetracene as for rubrene, only the 10%:40nm device was on par with the top two rubrene OLEDs, with an average EQE of approximately 0.12%.

Table 3.2.2 - Summary of Tetracene Doped OLEDs Performance

TPBi Thickness	40nm	60nm	80nm	100nm
Average EQE% [std dev; # data pts] at λ=550nm				
2%	0.0153 [0.003; 6]	0.0722 [0.045; 6]	0.0830 [0.016; 6]	0.0057 [0.002; 2]
10%	**0.1152 [0.011; 3]**	0.0454 [0.033; 3]	-	-
Turn on Voltage/V ± 1V				
2%	4-5	8-10	8-9	10
10%	5-6	7-9	-	-
Peak Wavelength:		**521nm**		

It is hypothesized that a similar dependence on final OLED thickness occurs in the tetracene devices as in the rubrene OLEDs. However, the tetracene doped films could exhibit different properties in the two tested concentrations which would result in a less efficient 2%:60nm device. Moreover, the absorbance of tetracene does not coincide as much with the P1 EL spectrum as does that of rubrene. Hence, the lower reported EQE values are in accordance with our initial expectations for the performance of the doped devices.

A separate experiment was conducted for the 2% tetracene OLEDs in which the TPBi thickness was increased to 80nm and 100nm. The reported EQE was 0.083% and 0.0057% respectively, suggesting that while an increase in the ETL thickness promotes EQE for tetracene, this is only up to a certain point, after which efficiency declines. It is noteworthy

that neither of these OLEDs functioned on par with the 10%:40nm tetracene device and EQE values higher than 0.1% were not attained for any of the 2% tetracene devices.

An interesting observation in Table 3.2.2 is the range of V_t values for the tetracene devices. While rubrene doped OLEDs exhibited turn on voltages similar to that of pure P1 devices of the same configuration (7-9V), V_t for tetracene OLEDs appeared to have more dependence on the thickness of the ETL. For thicker TPBi layers, V_t was noticeably higher; this is generally true for thicker devices.

It is postulated that the tetracene doped films could also differ in morphology from the rubrene doped films in terms of surface roughness and interaction with the P1 host. For very rough films, thinner TPBi layers could contain more defects which ultimately decrease the voltage drop across the ETL and reduce V_t. Furthermore, if aggregates of tetracene have formed in the emissive layer instead of dispersing evenly throughout, it is possible for electrons to bypass the P1 band gap and generate lower energy excitons on the band gap of the dopant. Both the surface roughness and phase interactions can influence V_t to vary, as is observed for the tetracene devices. Further investigation of the film morphology is required.

Figure 3.2.3 - Tetracene Doped OLED EL Spectrum

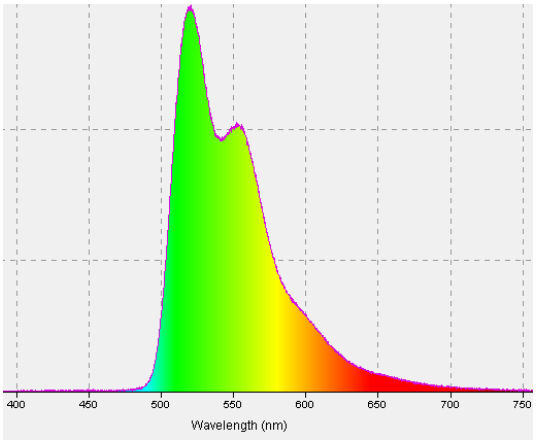

Like rubrene, tetracene doping caused a shift in the EL spectra from the broad double peaks of the blue-emitting P1 to a prominent 520nm peak with a small shoulder in the yellow region around 550nm. The ensuing implication is that

all P1 emission is transferred to the dopant, causing not only a change in the color of emitted light, but the efficiency as well.

Pentacene

Despite the trend for the previous two dopants, the highest performing pentacene device was the 10*%:60nm device followed by the 2*%:60nm OLED[6]. Neither of these functioned with EQE values similar to those of the other high performing devices. This result is in agreement with the initial assertion regarding spectral overlap between P1 emission and dopant absorption. Reduced energy available for excitation of the dopant molecules due to smaller overlap of P1 emission with pentacene absorption, translates to lower efficiency, as is evidenced by the values reported in Table 3.2.3. Furthermore, since the concentration of pentacene in the emissive layer was less than 2% and 10%, there might have been insufficient dopant molecules dispersed through the film. A lack of acceptors would certainly yield lower EQE compared to devices in which there is ample distribution of dopant in the host polymer.

Table 3.2.3 - Summary of Pentacene Doped OLEDs Performance

TPBi Thickness	**40nm**	**60nm**
Average EQE% [std dev; # data pts] at λ=625nm		
2*%	0.0077 [0.001; 4]	0.0156 [8E-4; 3]
10*%	0.0010 [5E-5; 2]	**0.0557 [0.026; 4]**
Turn on Voltage ± 1V		
2*%	6-7	6-7
10*%	7	7
Peak Wavelength/nm:	**622**	

[6] Recall that pentacene OLEDs were approximate 2% and 10%. Since the doped solution was saturated, actual weight concentrations were *less* than 2% and 10%.

Compared to the previous dopant recipes, it is possible that the 10*%:60nm is more similar to the 2%:60nm devices for rubrene and tetracene as the estimated concentration for 10*% pentacene films is less than 10%. In such a case, this highest performing pentacene recipe would actually coincide with the findings or prior doped OLEDs. For example, it may be more accurate to compare it with the top rubrene doped recipe of 2%:60nm which had an estimated EQE of 0.12%.

The turn on voltage for these devices did not appear to depend on thickness or dopant concentration. Yet, pentacene OLEDs did generally turn on at a lower voltage than pure P1 or rubrene devices. As previously mentioned, reduced V_t could originate from the properties of the spun emissive layer and its interaction with the adjacent ETL.

The EL spectra of pentacene devices included not only a salient peak in the vicinity 620nm, but some broad smaller peaks in the blue region as well. The presence of these peaks is evidence of the incomplete energy transfer from P1 to pentacene and to some extent explains the lower observed EQE of these OLEDs.

Figure 3.2.4 illustrates the EL spectra for the 4 pentacene recipes used. Of particular interest are the relative heights of the blue region peaks for the 2*% and 10*% spectra. Both devices made to 2*% exhibit higher emission in the blue region, which could arise from insufficient dopant

Figure 3.2.4 - Pentacene Doped OLEDs EL Spectra

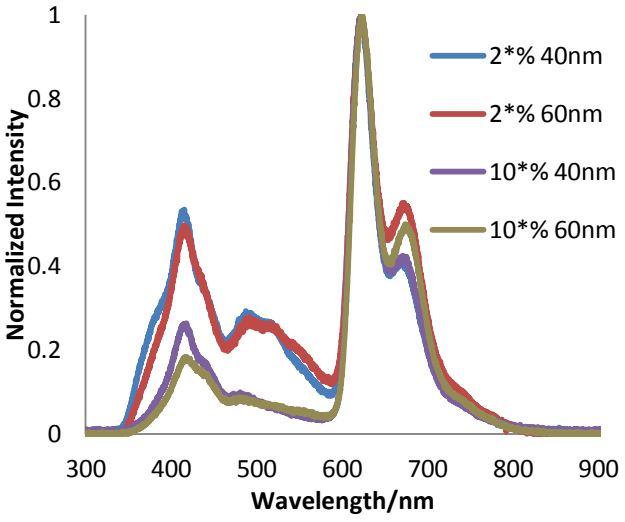

molecules within the emissive layer. The attenuated corresponding peaks for the 10*% spectra further support this hypothesis. From the findings reported in Table 3.2.3, it can be concluded that higher concentration of dopant not only abates blue emission but also enhances efficiency in the 60nm pentacene OLEDs.

Of the three dopants, pentacene prolonged the lifetime of the devices most extensively. Pads were switched on for upwards of 5 minutes with little noticeable color changes and minimal fading. It is deduced that pentacene has favorable interactions with the P1 host in this respect. Nevertheless, the 2*% and 10*%:40nm pentacene doped devices all eventually produced high intensity broad peaks in the 520nm region - a feature common to the TP and RP devices. It is suggested that some degradation of host P1 could be occurring with time, similar to what was observed for the undoped P1 OLEDs. Figure 3.2.5 shows the variation with time of the EL spectra for a 2*%:40nm pentacene device. Key features of this graph are the growing 520nm peak and diminishing 650nm peak suggestive of an overall degradation of the dopant and possibly the host as well.

Figure 3.2.5 - Time dependence of 2*%:40nm Pentacene OLED EL Spectra

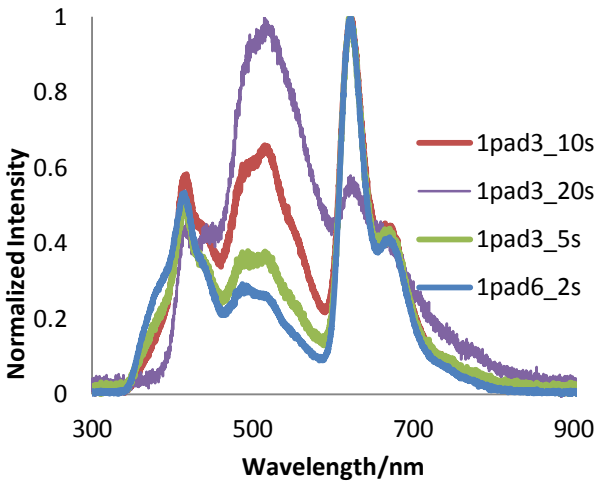

However, the 10*%:60nm device which exhibited the highest EQE of 0.056%, showed minimal signs of this EL shift after a prolonged period. Figure 3.2.6 illustrates this stability. This was not the case for the 10*%:40nm which had comparable behavior to that shown in Figure 3.2.5 after ≈4 minutes of being switched on.

It is noteworthy that whereas the 2*% devices produced the 520nm peak within 30s, 10*% devices lasted much longer before producing that feature. If the assumption is made that this green peak is associated with P1 degradation, it would appear that the dopants protect the host from such degradation. In this case, a higher concentration of dopant could deter the EL shift for longer. Analysis of EL spectra time dependence for the other dopants is necessary to confirm this hypothesis.

Figure 3.2.6 - Time Dependence of 10*%:60nm Pentacene OLED EL Spectra

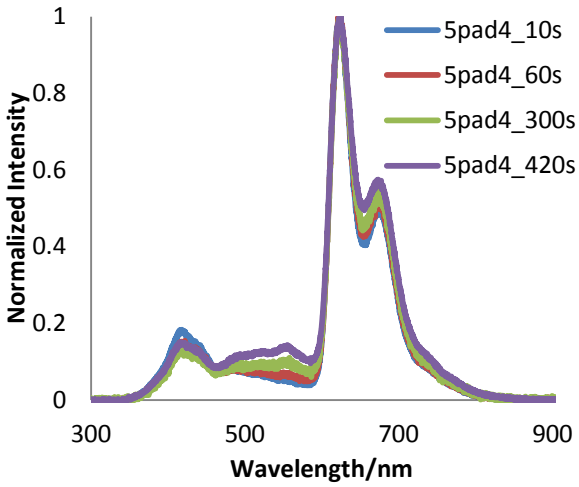

3.3. PEROXIDE OLEDS

Peroxide devices investigated in these experiments included 2% doped emissive layers and 60nm of TPBi. Both peroxide and UV treated doped devices were fabricated using 2% rubrene and tetracene, while pentacene was analyzed using only UV treated OLEDs of 2*% and 10*% concentrations. Parallel sets of OLEDs allowed for a direct comparison of the deposited endoperoxide with the treated acene so as to gauge the formation of peroxide from UV irradiation.

Figure 3.3.1 shows the EL spectra for all 6 peroxide recipes examined. Blue, green and red traces show the progression of spectra with time; blue representing the very first spectra and red, the last before the particular pad was turned off or malfunctioned. Time scales are relative and measurements were taken at approximate times shown.

Figure 3.3.1 - Time dependent EL Spectra of Peroxide OLEDs

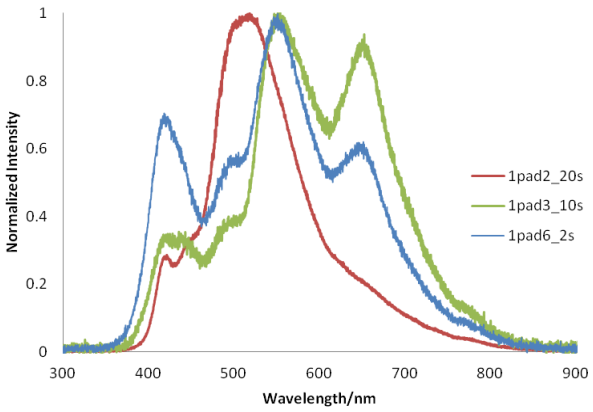

(a) 2% Rubrene Irr. in air

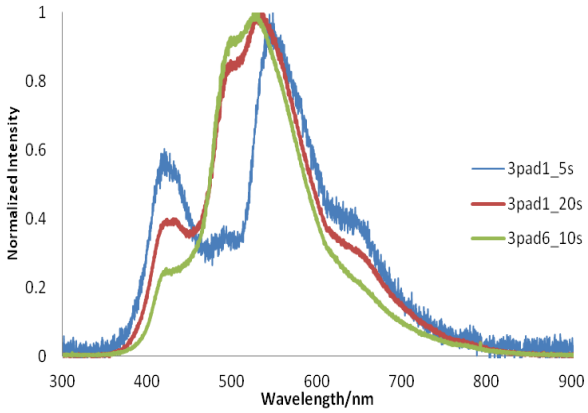

(b) 2% Rubrene Peroxide

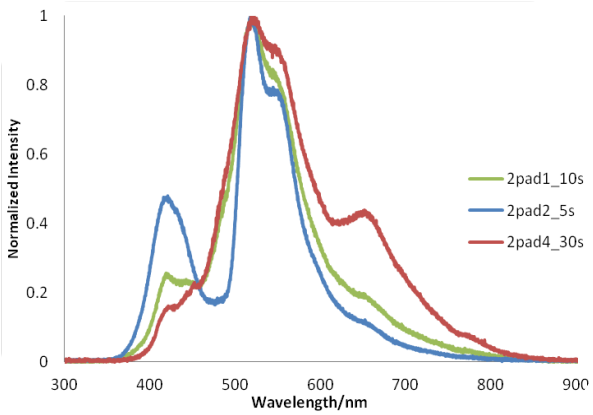

(c) 2% Tetracene Irr. in air

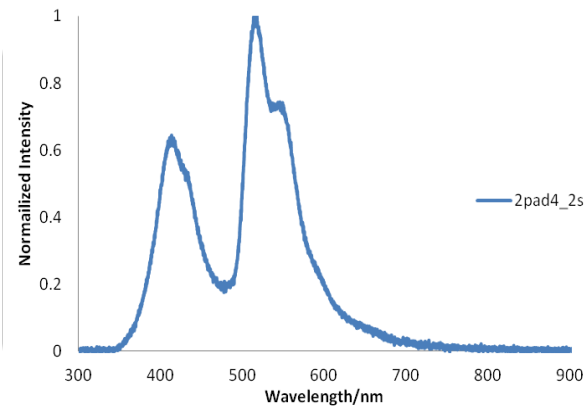

(d) 2% Tetracene Peroxide

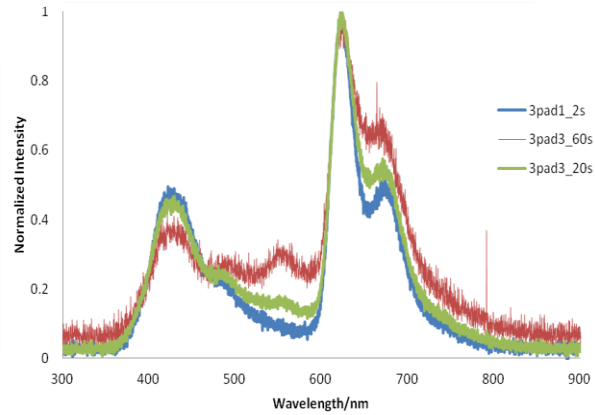

(e) 2*% Pentacene Irr. in air

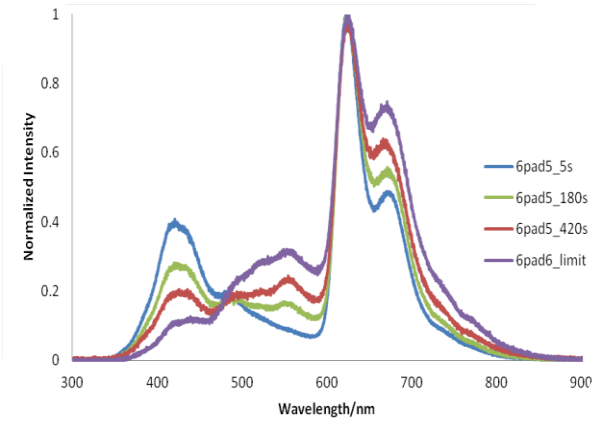

(f) 10*% Pentacene Irr. in air

Initial spectra for oxidized rubrene (RP) devices shown in (a) and (b) of Figure 3.3.1 include two major peaks which correspond to P1 (≈415nm) and rubrene (≈ 560nm). The presence of the former is indicative that the endoperoxide *does* have an effect on deactivating the color properties of the dopant. Comparing (a) and (b), it is seen that both spectra exhibit this behavior during the initial stages of turning on the devices and as time progresses, the intensity of the P1 peak decreases. In (a), there is initially a slightly more prominent peak around 650nm than in (b) which could indicate that complete dopant oxidation did not occur.

For tetracene peroxides (TP) the peak wavelengths occur at 415nm and 520nm while pentacene peroxides (PP) demonstrate peaks in the vicinity of 415nm and 620nm. Again, the 415nm peak suggests at least partial degradation of dopants to the endoperoxides occurred as purely doped devices register no remnants of the host in the EL spectra. The attenuation of the P1 peaks agrees with the expectation that current flow through endoperoxide devices severs the peroxide linkage to reform the un-oxidized dopants.

The diminishing P1 peak is also accompanied by a broadening green peak at approximately 520nm for both the RP and TP spectra and to a lesser degree, the PP spectra. It is possible that additional degradation of P1 occurred causing this growing peak similar to that found in pure P1 devices. RP and TP OLEDs also visibly appeared blue when turned on but quickly changed color to a pale green, corroborated by the broad peak in the 520nm region. This was not the case for the PP devices, which visibly exhibited constant color with time and concentration. In fact, the color emitted by the PP OLEDs was very similar to that of the pure pentacene doped devices and plots of the respective initial EL spectra on the same

Figure 3.3.2 - EL Spectra of 10*% Pentacene and PP OLEDs

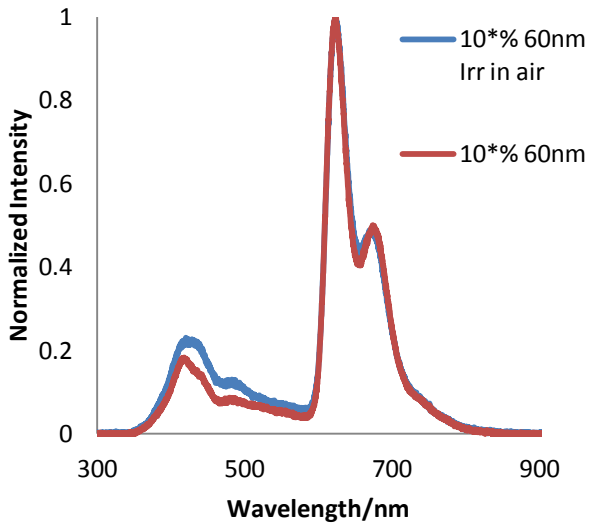

graph yield almost coinciding traces [Figure 3.3.2]. Color tunability was achieved in this respect, for the RP and TP but not PP devices. It is possible that the UV treatment was unsuccessful in generating the peroxide and that more extensive treatment is required. An alternative hypothesis is that the endoperoxide formed degenerates more readily than the other endoperoxides, rapidly yielding a pure pentacene doped device. Nevertheless, there was clearly some effect on the stability of the PP devices after UV treatment.

Graphs (e) and (f) both show that there is a gradual decay of the blue 415nm peak and a simultaneous growth in the smaller pentacene peak at 670nm. The growing 520nm attribute is less prominent than in the other peroxide spectra and in the pure pentacene doped devices, suggesting that the UV irradiation somehow improved the stability of the emission, despite ineffectively tuning the color.

RP and TP devices had poor life spans when turned on and EQE values on the order of 10^{-3}%, much like undoped P1 devices. For example, graph (d) of Figure 3.3.1 contains only one plot because that specific OLED expired quite rapidly after being turned on. On the contrary, PP devices demonstrated the best stability with time and were also able to retain color. The EQE of PP devices was in fact higher than the 2*% pentacene devices and on the order of the best performing pentacene device (EQE = 0.056%). The two PP recipes of 2*%

and 10*% had EQE of 0.022% and 0.041% respectively, indicating that UV treatment could actually enhance performance for low concentration emissive layers. Comparison with deposited pentacene endoperoxide devices is necessary for further conclusions.

4. CONCLUSIONS

In this research, color tunability of doped polyfluorene OLEDs was achieved for two of three acene dopants via UV treatment and exposure to singlet oxygen. It was found that for the particular experimental architecture employed in pure P1 devices, decreasing emissive layer thickness promoted EQE while increasing ETL thickness had the same effect. However restrictions on device thickness limit how thin or thick these respective layers can be fabricated.

Doping enhanced efficiency by two orders of magnitude and EQE in doped OLEDs emulated the degree of overlap between dopant absorption and host emission. As such, rubrene devices had the highest reported EQE values for two recipes: 2%:60nm and 10%:40nm. The tetracene devices were comparable in performance, with the 10%:40nm device exhibiting similar EQE to the top functioning rubrene OLEDs. Pentacene devices had the lowest EQE and also the lowest spectral overlap with P1 host emission. The best performing pentacene recipe was 10*%:60nm which is posited to be comparable to the 2%:60nm devices of other dopants by virtue of its true concentration (a value less than 10%). While all doped devices were more stable with time than undoped devices, pentacene OLEDs were particularly stable up to 7 minutes.

Experiments with the acene endoperoxides (rubrene and tetracene) produced EL spectra with different color attributes, namely the existence of P1 host peaks which were absent from purely doped device spectra. This is indicative of oxidation deactivating dopants thereby achieving color tunability. These devices however were not very stable with time and demonstrated EQE on the same order of undoped P1 OLEDs. Conversely, pentacene

peroxide devices became more stable after treatment and demonstrated relatively high efficiency similar to that of pure pentacene doped devices. Yet, there was no change in the observed color of pentacene peroxide devices and tunability was not accomplished for this dopant. It was posited that the peroxide was not generated for pentacene and if it was indeed produced, it did not persist for any significant time after the devices were switched on.

5. Future Work

Some areas of the research presented in this thesis require further investigations which can elucidate certain findings. For example, the effect of UV treatment in air on pure P1 films is also of interest as it could provide some insight to the behavior exhibited by the doped peroxide devices. Since time dependence data was not collected for preliminary devices, the EL spectral time dependence of undoped P1 devices would be beneficial as a means for explaining the growing 520nm peak in most fabricated OLEDs. Also, this data could be collected for the rubrene and tetracene doped OLEDs as well for comparison with the pentacene doped devices.

Another point of interest is the performance of penatcene peroxide devices fabricated with the endoperoxide instead of the dopant subjected to UV treatment. This could provide a useful comparison for the EL spectra and could verify whether or not the endoperoxide has an effect on the color emitted. Finally, the morphology of deposited layers, though not emphasized in this work, can be analyzed to better interpret layer thickness dependence and interfacial interactions.

BIBLIOGRAPHY

[1] Geffroy, Bernard, Philippe le Roy, Christophe Prat. "Organic light-emitting diode (OLED) technology: materials, devices and display technologies." *Polymer International* 55.6 (2006): 572-582. <http://onlinelibrary.wiley.com/doi/10.1002/pi.1974/pdf>.

[2] Kim, Sunkook, et al. "Low-Power Flexible Organic Light-Emitting Diode Display Device." *Advanced Materials* 23 (2011): 3511-3516.

[3] Sprengard, R, et. al. "OLED devices for signage applications - a review of recent advances and remaining challenges." *SPIE*. Bellingham, WA, 2004. <http://scitation.aip.org/getpdf/servlet/GetPDFServlet?filetype=pdf&id=PSISDG005519000001000173000001&idtype=cvips&doi=10.1117/12.567131&prog=normal>.

[4] "DisplaySearch: Flat panel growth to slow." *EE Times India* 24 October 2008. 15 March 2012. <http://www.eetindia.co.in/ART_8800549565_1800010_NT_bdc03eb7.HTM>.

[5] Tang, C.W., S. A. VanSlyke. "Organic electroluminescent diodes." *Applied Physics Letters* 51.12 (1987): 913-915.

[6] Gross, Markus, et al. "Improving the performance of doped -conjugated polymers for use in organic light-emitting diodes." *Nature* 405 (2000): 661-665.

[7] Chuo, Yindar, et al. "Towards Self-Powering Touch/Flex-Sensitive OLED Systems." *IEEE Sensors* 11.11 (2011): 2771-2779.

[8] Tong, Qing-Xiao, et al. "A High Performance Nondoped Blue Organic Light-Emitting Device Based on a Diphenylfluoranthene-Substituted Fluorene Derivative." *Journal of Physical*

Chemistry C 71.113 (2009): 6227-6230.

[9] Zhang, Jingjing, et al. "Structure, photophysics, and photooxidation of crowded diethynyltetracenes." *Journal of Materials Chemistry* 22.13 (2012): 6182-6189.

[10] Wood, V. C. *Electrical excitation of colloidally synthesized quantum dots in metal oxide structures*. PhD Thesis. Cambridge, MA: Massachusetts Institute of Technology, 2010.

[11] Sun, Yiru, et al. "Management of singlet and triplet excitons for efficient white organic light-emitting devices." *Nature* 440 (2006): 908-912.

[12] Sun, Sam-Shajing and Larry, R. Dalton. *Introduction to Organic Electronic and Optoelectronic Materials and Devices*. Boca Raton: CRC Press, 2008.

[13] *Extending the Lifetimes of OLEDs Through an Improved Sealing Process*. n.d. Georgia Tech Research Institute. <http://www.gtri.gatech.edu/casestudy/improving-oled-lifetimes>.

[14] "Chemwiki," UC Davis, [Online]. Available: http://chemwiki.ucdavis.edu/@api/deki/files/5318/=dex1.PNG.

[15] Nave, C.R. *Hyper Physics - Work Functions for Photoelectric Effect*. 2012. Georgia State University. <http://hyperphysics.phy-astr.gsu.edu/hbase/tables/photoelec.html>.

[16] Ma, Zhu, et al. "Non-doped white organic light-emitting diodes consisting of three primary colors based on a bipolar emitter." *Displays* 33.1 (2012): 42-45.

[17] Miteva, Tzenka, et al. "Annihilation assisted upconversion: all-organic, flexible and transparent multicolour display." *New Journal of Physics* 10 (2008): 103002.

APPENDIX A

Summary of Forster energy transfer which occurs in doped emissive layer of OLEDs [14].

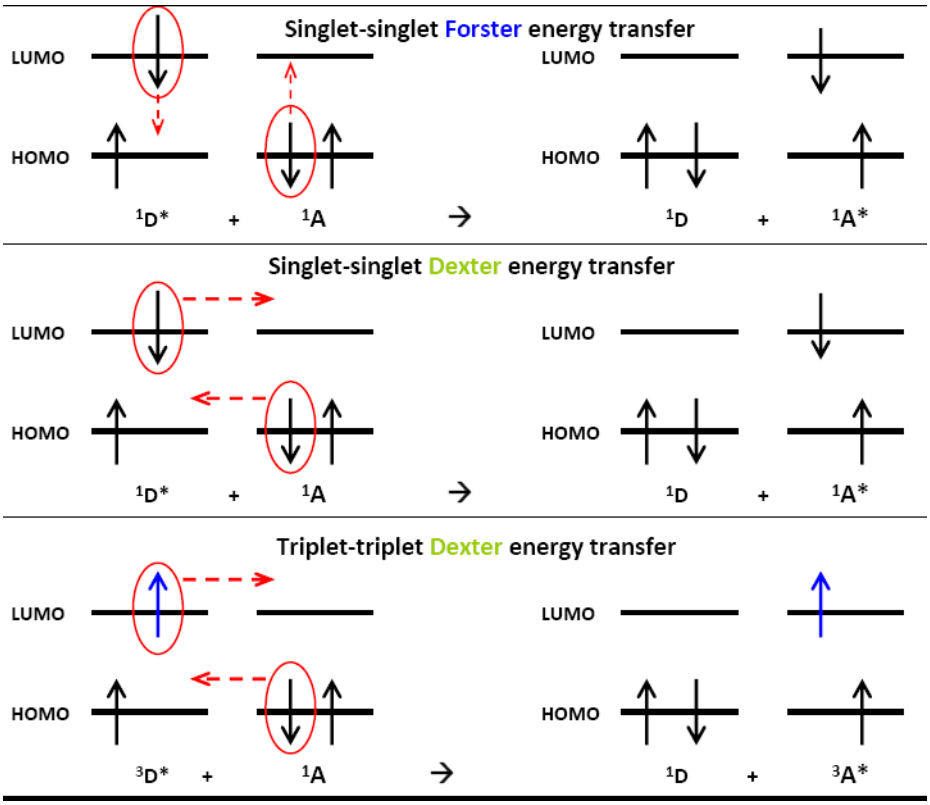

APPENDIX B

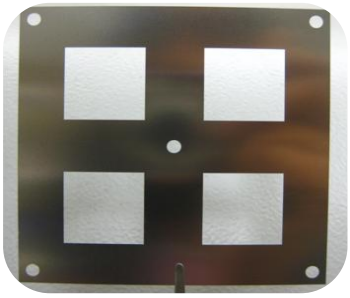

(a) Mask for ETL deposition (4 substrates)

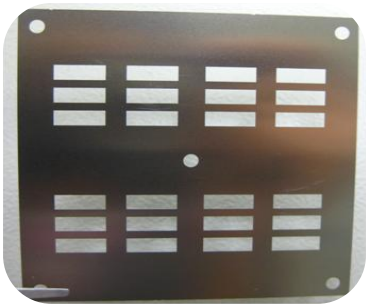

(b) Mask for electrode deposition (4 substrates)

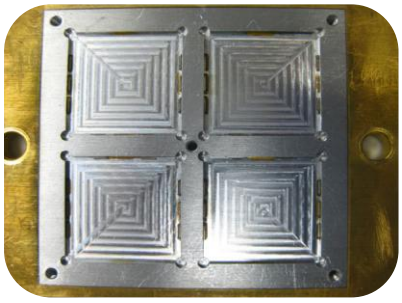

(c) Loading base for thermal evaporation vacuum chamber

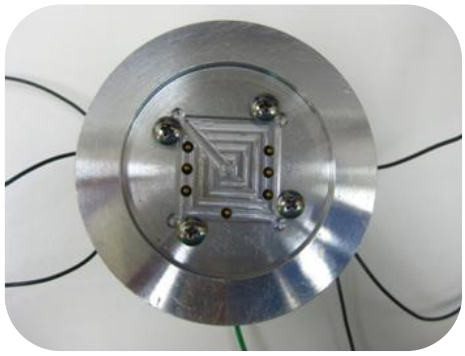

(d) OLED testing apparatus

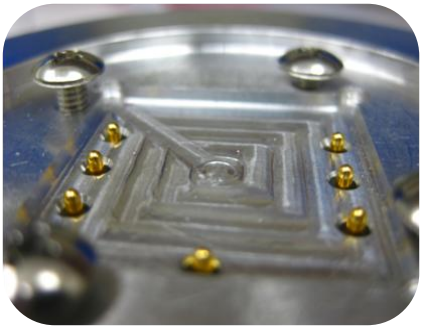

(e) Contact pins for electrodes on testing apparatus

APPENDIX C

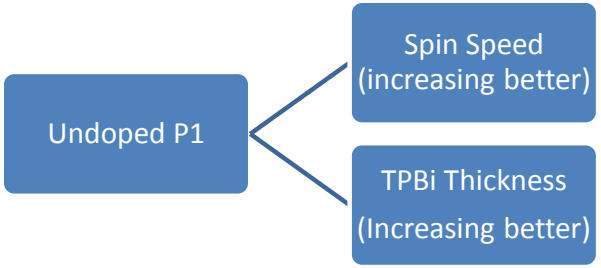

Doped P1

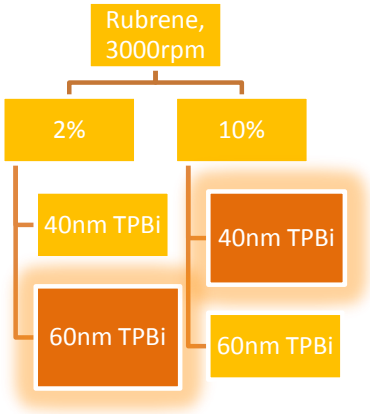

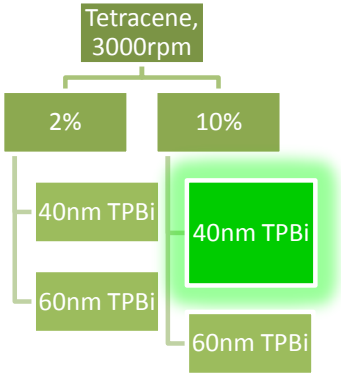

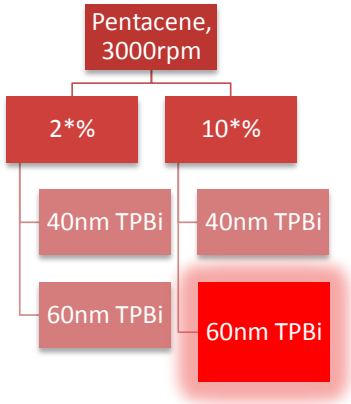

Doped Peroxides